Carbohydrate Polymers 121 (2015) 190–198

Contents lists available at ScienceDirect

Carbohydrate Polymers

journal homepage: www.elsevier.com/locate/carbpol

Aptamer decorated hyaluronan/chitosan nanoparticles for targeted delivery of 5-fluorouracil to MUC1 overexpressing adenocarcinomas

Zahra Ghasemi[a], Rassoul Dinarvand[b], Fatemeh Mottaghitalab[b], Mehdi Esfandyari-Manesh[b], Elmira Sayari[a], Fatemeh Atyabi[a,*]

[a] Dept. of Pharmaceutical Nanotechnology, Faculty of Pharmacy, Tehran University of Medical Sciences, Tehran 14174, Iran
[b] Nanotechnology Research Centre, Faculty of Pharmacy, Tehran University of Medical Sciences, Tehran, Iran

ARTICLE INFO

Article history:
Received 17 August 2014
Received in revised form 2 December 2014
Accepted 4 December 2014
Available online 31 December 2014

Keywords:
Chitosan
Hyaluronan
MUC1-binding aptamer
5-Fluorouracil

ABSTRACT

An aptamer (Apt) conjugated hyaluronan/chitosan nanoparticles (HACSNPs) were prepared as carrier for targeted delivery of 5-fluorouracil (5FU) to mucin1 (MUC1) overexpressing colorectal adenocarcinomas. Nanoparticles had about 181 nm size, encapsulation efficiency of 45.5 ± 2.8 and acceptable stability. Conjugation of MUC1-binding Apt to the surface of the nanoparticles was confirmed by gel electrophoresis. Toxicity and cellular uptake of nanoparticles were investigated by *in vitro* cytotoxicity assays and confocal scanning microscopy in ($MUC1^+$) human adenocarcinoma and ($MUC1^-$) Chinese hamster ovary cells. Toxicity of nanoparticles were significantly higher in comparison with free drug in both cell lines while this rising was more efficient for nanoparticles decorated with Apt in $MUC1^+$ cell line. The same result was observed in the cellular uptake study. It could be concluded that the present system has the potential to be considered in treatment of $MUC1^+$ colorectal adenocarcinomas.

© 2015 Elsevier Ltd. All rights reserved.

1. Introduction

It is believed that nanoparticulate drug carriers passively accumulate into tumor sites due to their abnormally leaky vasculature and lack of effective lymphatic drainage system (Duncan, 2003). A wide range of materials have been employed as drug carriers. Among these, low molecular weight chitosan has shown remarkable advantages as colloidal drug carrier due to its high water solubility, bioadhesive and absorption enhancing properties (Jarmila & Vavrikova, 2011). More recent approaches have exploited the addition of hyaluronan (HA) to chitosan-based nanoparticles (Muzzarelli, Stanic, Gobbi, Tosi, & Muzzarelli, 2004; Muzzarelli, Greco, Busilacchi, Sollazzo, & Gigante, 2012). It seems that combination of high mucoadhesive property of hyaluronan and penetration enhancing effect of chitosan, make hyaluronan/chitosan nanoparticles (HACSNPs) superior to the drug delivery systems. Many studies, suggest that the inclusion of hyaluronan has provided gene and drug delivery systems with improved, synergistic properties through reduction of non-specific interaction between HACSNPs and serum proteins and at the same time improvement of their internalization to cells expressing CD44, Hyaluronan-mediated motility receptor (RHAMM), or hyaluronic acid receptor on liver endothelial cells (HARLEC) receptors (Mok, Park, & Park, 2007).

To overcome the limitations of the passive targeting, there have been considerable efforts devoted to the preparation of nanoparticles bearing tumor-targeting moieties (Bae & Park, 2011). MUC1 mucin is a large transmembrane glycoprotein with good immunogenic properties, which its expression increased at least 10-fold in most malignant adenocarcinomas making it an ideal target molecule for chemotherapeutic.

Nucleic acid aptamers (Apts) are single-strand oligonucleotides that could form unique tridimentional structures and possess advantages like low synthesis cost, low immunogenicity and small size (Bertrand, Wu, Xu, Kamaly, & Farokhzad, 2014). *In vitro* feasibility of Apt-decorated nanoparticles as a cancer marker to target the prostate specific membrane antigen (PSMA) was reported in 2004. Since then, various authors have studied the efficacy of Apt targeted nanoparticles against PSMA and described efficacy of the system in decreasing the tumor growth and the survival increasing *in vivo* (Farokhzad et al., 2006).

In order to target MUC1 tumor marker, Ferreira et al., have developed several Apts that could bind to MUC1 positive tumor cells based on systematic evolution of ligands by exponential enrichment (SELEX) methodology. They evaluated the binding affinity and selectivity of designed Apts against MUC1 and reported high

* Corresponding author. Tel.: +98 21 66959052; fax: +98 21 66959052.
E-mail address: atyabifa@tums.ac.ir (F. Atyabi).

http://dx.doi.org/10.1016/j.carbpol.2014.12.025
0144-8617/© 2015 Elsevier Ltd. All rights reserved.

affinity of obtained Apts against MUC1 glycoprotein(Ferreira, Matthews, & Missailidis, 2006). It has been shown that the MUC1-binding Apts could be employed to selectively deliver phototherapy agent to cancer cells (Ferreira, Cheung, Missailidis, Bisland, & Gariepy, 2009). Later studies indicated the potentials of MUC1-binding Apts in high-sensitive detection and collection of MCF-7 breast cancer cells (Chang et al., 2014).

In this study, we prepared a nanocarrier system based on the combination of hyaluronan and low molecular weight chitosan. MUC1-binding Apt was conjugated to the surface of the nanoparticles for promoting active targeting of the anticancer 5FU. The basic properties of HACSNPs as drug carrier and its role as vehicle in drug cytotoxicity was studied. We evaluated *in vitro* delivery efficiency by comparing cytotoxicity and cellular uptake of non-targeted and Apt-targeted formulations in HT-29 colorectal adenocarcinoma cell line and CHO cells.

2. Materials and methods

2.1. Materials

Hyaluronan (M_W 10 kDa) was purchased from Guanglong Biochem, (ShanDong, China). Chitosan [Low molar mass, 96% deacetylation] was supplied from Primex (Karmoy, Norway). 5-fluorouracil (purity >99%) and cumarin-6 were purchased from Sigma-Aldrich, (St. Louis, MO, USA). 72 base pair MUC1-binding DNA aptamer (Apt) with sequence of (5′-Amino-C_6-GGG AGA CAA GAA TAA ACG CTC AAG AAG TGA AAA TGA CAG AAC ACA ACA TTC GAC AGG AGG CTC ACA ACA GGC-3′) was ordered to TAG Copenhagen A/S, (Copenhagen, Denmark). HT-29 and CHO cell lines were provided by National cell bank of Pasteur Institute, (Tehran, Iran). Other reagents, chemicals and solvents were of analytical grade.

2.2. Depolymerization of chitosan

Low molecular weight chitosan was prepared according to the depolymerization method described previously. Briefly, 10 mL sodium nitrite solution (1 mg/mL) was added to 100 mL solution of chitosan 2% (W/V) in 6% (V/V) acetic acid and allowed to proceed for 1 h while stirring. Afterward, pH of the reaction raised to 9 by adding NaOH (5 N) dropwise. The precipitated white-yellowish depolymerized chitosan was filtered and washed with acetone. The product redissolved in acetic acid 0.1 N and then dialysis against deionized water (2 × 2 L for 90 min and 1 × 2 L overnight). The dialyzed product was lyophilized at 50 °C and 10 Pa (LyoTrap plus, LTE Scientific, Chorley, United Kingdom) and kept for further usage.

2.3. Molecular weight measurement

The molecular weight of depolymerized chitosan was measured as previously described by our group (Sayari et al., 2014) using static light scattering (SLS). SLS is a technique to measure molecular weight using the relationship between the intensity of light scattered by a molecule and its molecular weight and size, as described by the Rayleigh theory (Muzzarelli, Lough, & Emanuelli, 1987). Three different concentrations of depolymerized chitosan were prepared and time-averaged intensity of scattered light and average molecular weight was measured by Zetasizer ZS, (Nano-ZS, Malvern, Worcestershire, UK).

2.4. HACSNPs preparation

Nanoparticles were prepared by a spontaneously ionotropic gelation between the positively charged amino groups of chitosan and the negatively charged carboxyl groups of hyaluronan. 10 mL of an aqueous solution of hyaluronan (0.8 mg/mL) containing 5 mg 5FU were dropped into 10 mL of an aqueous solution of chitosan (1.2 mg/mL, pH 5, adjusted by acetic acid 1% V/V) under magnetic stirring (400 rpm) at room temperature. The solution was kept stirring for 30 min. Then, the nanoparticles were centrifuged with 20 μL of a glycerol bed at 21,000 rpm for 30 min. The sediments resuspended in 10 mL deionized water. This procedure was repeated once without glycerol bed and the product was freeze-dried for future work.

2.5. Encapsulation and loading efficiency

In order to determine the encapsulation efficiency (EE) and loading capacity (LC) of selected formulations, nanoparticles were isolated by centrifugation (21,000 rpm, 30 min, 25 °C) without a glycerol bed. The supernatants were collected and amounts of unbounded drug were measured spectroscopically at 266 nm using UV spectrophotometer (Scinco S-3100, Seoul, Korea). The EE and LC were calculated using the following equations:

$$\text{Encapsulation efficiency} = \frac{\text{total amount of drug} - \text{amount of unbounded drug}}{\text{total amount of drug}} \times 100$$

$$\text{Loading capacity} = \frac{\text{total amount of drug} - \text{amount of unbounded drug}}{\text{weight of nanoparticles}} \times 100$$

2.6. Characterization of nanoparticles

The hydrodynamic mean diameter, zeta potential and polydispersity index (PDI) of the nanoparticles were determined by dynamic light scattering (DLS) using the aforementioned Zetasizer. The shape and surface morphology of nanoparticles before and after loading of 5FU were characterized by scanning electron microscope (XL 30, Philips, Eindhoven, Netherlands).

2.7. FTIR study

Fourier Transmission Infrared (FTIR) study was performed in order to assess the presence of hyaluronan, chitosan and 5FU in nanoparticles using Nicolet spectrometer (Nicolet Magna IR 550, Madison, WI). The Samples were mixed with KBr and scanned in the spectral region of 4000–400 cm^{-1}.

2.8. XRD analysis

Molecular arrangement of 5FU in nanoparticles was assessed by XRD analysis. Powder X-ray diffraction pattern of samples were obtained at room temperature using X-ray diffractometer (Siemens, Germany) with Cu Kα radiation. The data were collected over an angular range from 3° to 60° 2θ in continuous mode using a step size of 0.04° 2θ.

2.9. In vitro drug release

Drug release was studied in phosphate buffered saline medium (PBS; pH 7.4 and 5.5). Briefly, 35 mg of freeze-dried 5FU loaded HACSNPs was dispersed in the medium and placed into dialysis bag (M_W cut off 12 kDa, Sigma-Aldrich GmbH, Germany). The dialysis bag was incubated in 50 mL of PBS at 37 °C and shaken at 100 cycles/min. At the predetermined time intervals, 2 mL of the medium was collected for 5FU analysis by UV spectrophotometry and equivalent volume of fresh PBS solution was supplemented in order to keep the volume of the system identical.

2.10. Stability study

The physical stability of the nanoparticles was evaluated in primary aqueous suspension and PBS buffer (pH 5.5 and 7.4) upon storage at room temperature. Prepared nanoparticles were centrifuged in the presence of glycerol bed fallowed by dispersion in the media. At periodical intervals, samples took out from each medium and the particle size, zeta potential and PDI of the samples were determined as mentioned above.

2.11. Conjugation of MUC1-binding Apt

The conjugation of MUC1-binding Apt to the surface of nanoparticles was accomplished via activation of carboxyl groups of hyaluronan by 1-ethyl-3-(3-dimethylaminopropyl) carbodiimide and *N*-hydroxysuccinimide (EDC/NHS technique) (Dhar, Gu, Langer, Farokhzad, & Lippard, 2008). Drug loaded HACSNPs was suspended in DNase/RNase free water (5 μg/μL, 250 μL) and incubated with excess aqueous solutions of EDC (400 mM, 100 μL) and NHS (100 mM, 100 μL) at room temperature for 30 min. The resulted *N*-hydroxysuccinimide-activated nanoparticles washed with DNase/RNase free water by ultrafiltration (5000 × *g*, 10 min, Ultracel membrane, 30,000 MWCO, Amicon, Millipore Corporation, Bedford, USA) to remove the residual EDC and NHS. The activated nanoparticles were reacted with 5′-NH_2-modified MUC1-binding Apt (1 μg/μL, in DNase/RNase free water, 25 μL) for 3 h at room temperature. Apt conjugated nanoparticles were purified by centrifugation (2 × 10 min, 16,000 × *g*, 5 °C).

2.12. Agarose gel electrophoresis

Conjugation of the MUC1-binding Apt to the surface of nanoparticles was confirmed by agarose gel electrophoresis. Gel electrophoresis was performed using 2% (W/V) agarose gel in a 1 M Tris-acetate-EDTA (TEA buffer) solution. HACSNPs and Apt-coupled HACSNPs before and after purification were mixed by 2 μL of the loading dye and loaded onto the gel while free MUC1-binding Apt was used as control. The samples were subjected to 110 V for 20 min. Then, the gel was incubated in 0.5% gel red solution for further 20 min and visualized under UV illumination.

2.13. Cytotoxicity assay

A series of 3-(4,5-dimethylthiazol-2-yl)-2,5-diphenyltetrazolium bromide (MTT) based assays were performed for comparing the anti-cancer capability of the free 5FU, the non-targeted and Apt-targeted HACSNPs, using ($MUC1^+$) HT-29 and ($MUC1^-$) CHO cell lines. The cells (1×10^5 cells/mL) were seeded into 96-well plate and incubated at 37 °C. After 24 h, cells were treated by various formulations at the drug concentration of 1.25, 2.5, 5, 10, 20 and 40 μg/mL. Plates were incubated in a humidified 5% CO_2 balanced-air incubator at 37 °C for 24, 48 and 72 h. At the designated intervals, old medium was removed and 200 μL fresh medium which was contained 0.5 mg/mL MTT has been added to the wells. Plates were incubated for another 4 h at 37 °C and 5% CO_2. The medium was then replaced with 50 μL dimethyl sulfoxide (DMSO). Finally, the absorbance was read with a plate reader (BioTek ELX800, USA), at the wavelength of 570 nm. The percentage of cell viability was calculated by the following equation:

$$\%\ \text{cell viability} = \frac{\text{Abs}_{\text{sample}}}{\text{Abs}_{\text{control}}} \times 100$$

where $\text{Abs}_{\text{sample}}$ is the absorbance of cells tested with various formulations and $\text{Abs}_{\text{control}}$ is the absorbance of control cells which incubated with cell culture medium only.

2.14. In vitro cellular uptake

The cellular uptake of non-targeted and Apt-targeted HACSNPs by HT-29 and CHO cells were studied through confocal fluorescence scanning microscopy (CFSM). Cells were cultured under 5% CO_2 and 95% relative humidity at 37 °C. The cells were allowed to adhere to a glass cover slip in 6-well plate for 24 h. The medium was removed and the cells were incubated with 100 μg/mL non-targeted and Apt-targeted HACSNPs, both containing cumarin-6 for 4 h. Cumarin-6 loaded nanoparticles were prepared following the previously described in Section 2.4. Afterward, the cells were washed 3 times with PBS and were incubated with DAPI for 5 min in order to staining the nuclei and rewashed 3 times with PBS. The cells were then fixed with 1% formaldehyde for 10 min at 4 °C and analyzed by CFSM.

2.15. Statistical analysis

Unpaired student's t test used for between two-group comparison and one-way ANOVA with Fisher's LSD for multiple-group analysis. A probability (*P*) less than 0.05 was considered statistically significant.

3. Results and discussion

3.1. Formulation variables for nanoparticles preparation

HACSNPs loaded with 5FU were prepared by iontropic gelation technique. In order to increase and optimize the encapsulation efficiency, as a simple resolution, total polymer concentration was increased. Table 1 summarizes the effect of increasing the total polymer concentration on drug encapsulation efficiency and size of nanoparticles. Generally, increasing the total polymer concentration from 0.1 mg/mL to 1 mg/mL resulted in increasing the encapsulation efficiency and size of nanoparticles. Applying polymer concentration higher than 1 mg/mL caused precipitation during preparation. Umerska et al. (2012), studied assembly process and properties of cross-linker free HACSNPs and reported higher yield of particle formation and turbidity and increasing the size of nanoparticles with positive zeta potential following using higher concentration of polymer. Their finding is in agreement with our study.

Furthermore, it was observed that pH variations could affect the assembling characteristics of HACSNPs. It is considered that amino groups of chitosan could be protonated in low pH which can lead to better interaction between chitosan and hyaluronan. Nevertheless,

Table 1
Effect of total polymer concentration on size and encapsulation efficiency. Amount of 5FU, chitosan/hyaluronan ratio of 3:1 and total volume of 20 mL were kept constant. (mean ± S.D., $n = 3$).

Total polymer conc. (mg/mL)	Size (nm)	Encapsulation efficiency (%)
0.1	124 ± 5.0	11.5 ± 0.9
0.2	127 ± 2.0	13.9 ± 1.1
0.3	131 ± 4.0	14.4 ± 0.2
0.4	139 ± 2.0	16.4 ± 0.9
0.5	145 ± 3.0	16.9 ± 0.1
0.6	165 ± 2.0	22.0 ± 3.2
0.7	168 ± 7.0	24.1 ± 0.4
0.8	170 ± 6.0	33.5 ± 2.0
0.9	178 ± 7.0	41.1 ± 1.7
1	182 ± 3.0	47.3 ± 1.0

Table 2
Effect of polymer mixing ratio on size, PDI, zeta potential and encapsulation efficiency. Amount of 5FU, total polymer concentration of 1 mg/mL and total volume of 20 mL were kept constant. (mean ± S.D., $n = 3$).

% Chitosan	% Hyaluronan	Size (nm)	PDI	Zeta potential (mV)	Encapsulation efficiency (%)
95	5	133 ± 5.0	0.15 ± 0.0	26 ± 0.4	11.5 ± 0.8
90	10	137 ± 2.0	0.14 ± 0.0	24 ± 0.2	15.0 ± 1.3
85	15	140 ± 1.0	0.14 ± 0.0	22 ± 0.5	20.6 ± 1.0
80	20	147 ± 1.0	0.13 ± 0.0	21 ± 0.3	25.5 ± 1.1
75	25	150 ± 2.0	0.13 ± 0.0	19 ± 0.5	29.7 ± 0.5
70	30	152 ± 3.0	0.12 ± 0.0	18 ± 0.3	33.0 ± 1.7
65	35	166 ± 4.0	0.11 ± 0.0	16 ± 0.5	37.7 ± 1.2
60	40	181 ± 2.0	0.09 ± 0.0	15 ± 0.4	45.5 ± 2.8

in pH bellow 3.5, reduction of negatively charged groups of hyaluronan lower its interaction with chitosan which leads to the creation of bigger nanoparticles. Besides of all the mentioned observations, the acidic nature of 5FU may lessen its solubility and assist more inclinations to entrapment into the polymers matrix. Therefore, pH about 5 was employed in all HACSNPs formulations.

Table 2 represents the effect of different amounts of hyaluronan and chitosan on size, PDI, zeta potential and loading efficiency of the nanoparticles. In general, lowering the amount of the applied hyaluronan (less than 10% of total polymer concentration) causes low loading efficiencies. Besides the loading efficiency, increasing the amount of hyaluronan augments the size of nanoparticles as well. However, increasing the hyaluronan content to more than 40% of total polymer concentration led to instability and precipitation in the system. These observations can be explained through the fact that interaction between positively and negatively charged groups forms the nanoparticles. When the amount of hyaluronan as polyanion was very low, the quantity of formed nanoparticles was also low and lead to low drug encapsulation. Increasing the amounts of hyaluronan causes more assembling of negatively and positively charged chains and as a result higher nanoparticle formation and drug entrapment. This buildup indeed depends on the charge mixing ratio (CMR) of the polymers. Once the CMR of the polymers approaching 1, opposite charges are neutralized and the aggregation and phase separation expected to occur (Nizri, Magdassi, Schmidt, Cohen, & Talmon, 2004). The positive zeta potential of all stable formulations indicates that the surface of nanoparticles is preferably composed of chitosan. Anyhow, zeta potential of the nanoparticles decreased from 26 to 15.3 with increasing amount of hyaluronan in total polymer concentration from 5% to 40%, respectively. This reduction points to the presence of the negatively charged carboxyl groups of hyaluronan on the surface of the nanoparticles and more complexes between positive and negative groups of chitosan and hyaluronan. The PDI decreased with increasing amounts of hyaluronan. Relationship between increasing amounts of hyaluronan and PDI has been showed variable results in previous studies. Most of the studies on using HACSNPs as gene delivery system have reported higher PDI with increasing amounts of hyaluronan (Duceppe & Tabrizian, 2009) while study on cross-linker free HACSNPs described lower PDI with increasing hyaluronan for nanoparticles with positive surface charge (Umerska et al., 2012). One of the probable reasons for these controversial observations may be the presence of DNA and TPP molecules and repulsion forces between DNA, TPP and hyaluronan in gene delivery studies.

For furthered studies, the formulation containing 12 mg chitosan, 8 mg hyaluronan and 5 mg 5FU was selected due to high encapsulation efficiency of 5FU and acceptable size, zeta potential and PDI.

3.2. Morphology studies

The particle size and size distribution of optimized 5FU loaded HACSNPs were about 181.3 ± 2.3 and 0.096, respectively. The SEM images proved that nanoparticles have uniform spherical shape and narrow size distribution before and after drug loading. It seems that encapsulation of 5FU had no significant effect on surface morphology of the nanoparticles but a little larger size of drug loaded nanoparticles could be due to increasing ionic interaction between positively charged 5FU and chitosan and negatively charged HA chains after presence of drug (Fig. 1).

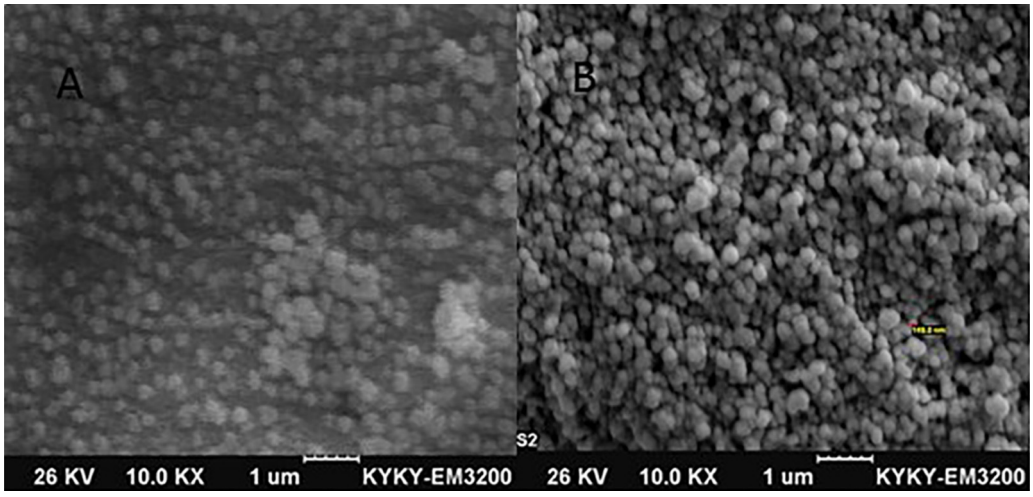

Fig. 1. Surface morphology of optimized 5FU loaded HACSNPs by scanning electron microscopy (SEM). (A) Blank nanoparticles, (B) 5FU loaded nanoparticles.

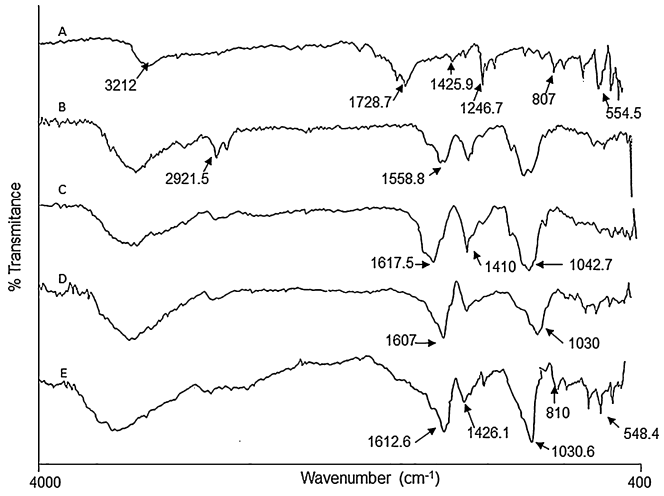

Fig. 2. FTIR spectra of (A) 5FU, (B) chitosan, (C) hyaluronan, (D) blank nanoparticles and (E) 5FU loaded HACSNPs.

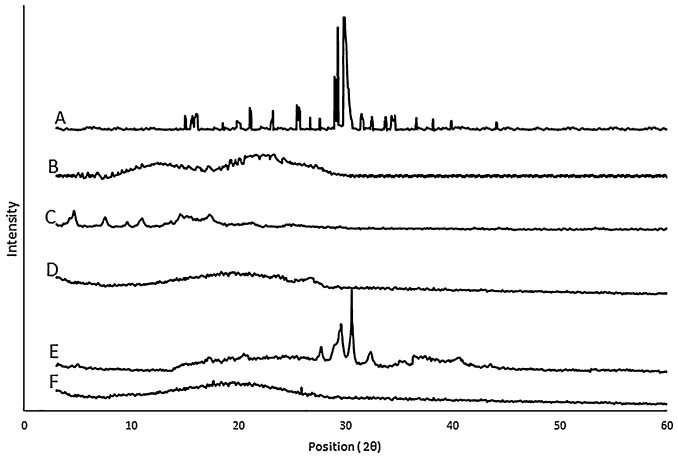

Fig. 3. XRD diffractograms of (A) 5FU, (B) depolymerized chitosan, (C) hyaluronan, (D) blank nanoparticles, (E) physical mixture of 5FU and blank nanoparticles and (F) 5FU loaded HACSNPs.

3.3. FTIR analysis

As shown in Fig. 2A, characteristic peaks at 3212, 1728.7, 1425.9, 1246.7, 807.9 and 554.5 cm^{-1} are detected due to the vibration of imide stretch and aromatic ring in the structure of 5FU. Spectrum of chitosan (Fig. 2B) shows the intense peaks at 1086 cm^{-1} due to C—O stretching of ether group and peak at 1558.8 cm^{-1} confirms the presence of amide II. hyaluronan shows sharp peaks

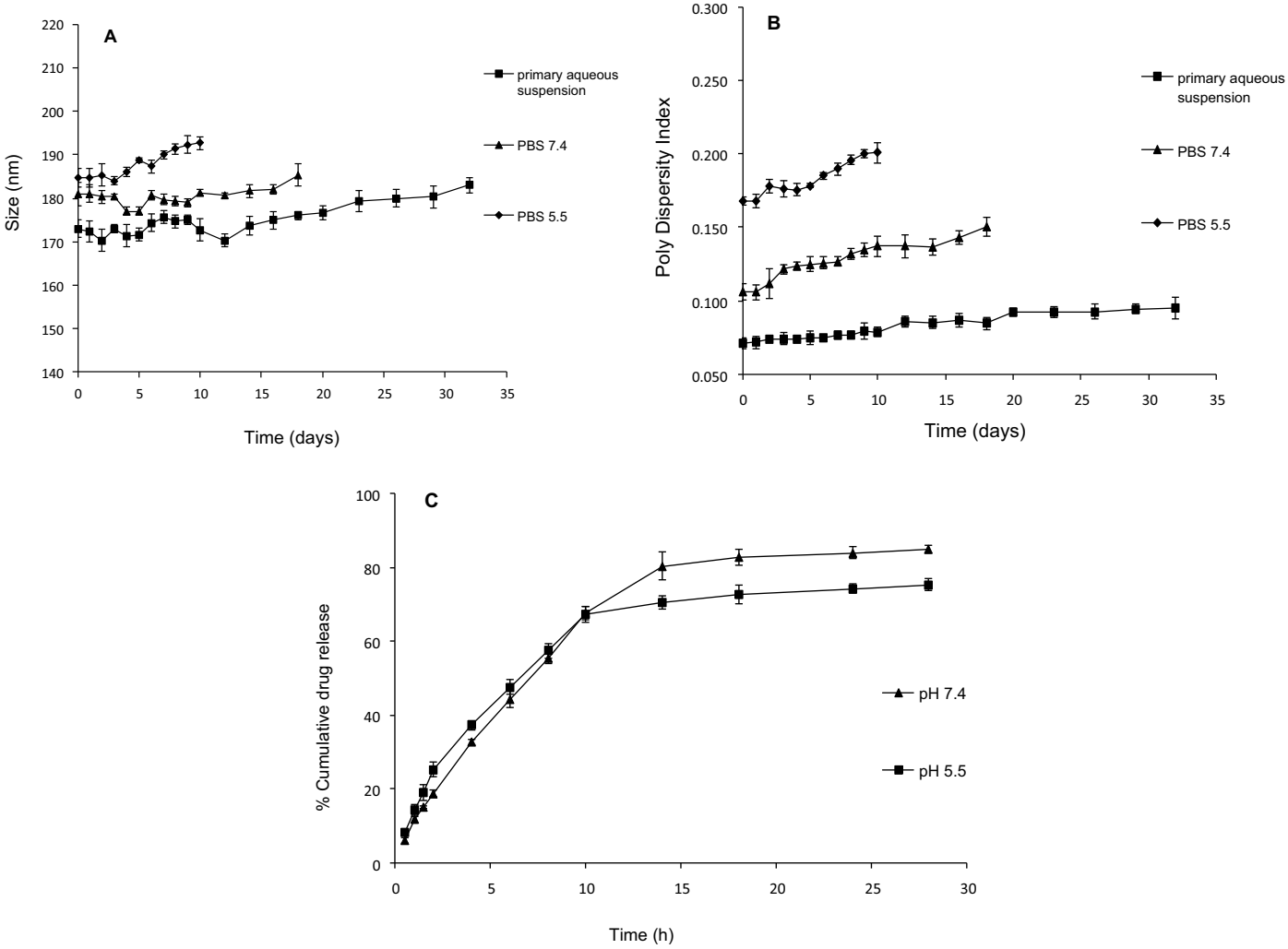

Fig. 4. Variations of (A) size and (B) PDI of the 5FU loaded HACSNPs (■) in primary aqueous suspension, (▲) in PBS pH 7.4 and (♦) PBS pH 5.5. (C) In vitro drug release profile of 5FU loaded HACSNPs, (■) in PBS pH 5.5 and (▲) in PBS pH 7.4.

at 1042.7 cm^{-1}, 1410 cm^{-1} and 1617.5 cm^{-1} that could be due to the C—O—C stretching, the presence of C—O groups with C=O combination and the presence of amide II group, respectively (Fig. 2B). In the case of blank HACSNPs and 5FU loaded HACSNPs, shifting amide II peak of chitosan and C—O—C stretching of hyaluronan to around 1600 cm^{-1} and 1030 cm^{-1} respectively, could indicate the ionic interaction between positively charged chitosan and negatively charged hyaluronan (Li, Wang, Peng, She, & Kong, 2011). Besides, presence of 5FU related peaks at 1426.1, 810 and 548.4 cm^{-1} in 5FU loaded HACSNPs and absence of these peaks in blank HACSNPs, indicated that 5FU was encapsulated in nanoparticles and intramolecular interaction is generally of electrostatic nature.

3.4. XRD analysis

X-ray diffractometry provides valuable data about physical state and type of dispersion of a drug in a polymer matrix. As it shown in Fig. 3IA diffractogram of 5FU exhibited intense peak at 2θ values of 15.98, 21.6, 23.58, 29.5, 30.08, 31.82, 39.74 and 45.88 due to its crystalline nature. Intense peaks also were observed for pure HA at 5.62, 8.58, 10.02, 12.44 and 18.72 because of using sodium salt of this polymer (Fig. 3IB) while freez-dried depolymerized low molecular weight chitosan showed wide peaks at about 12.62 and 23.48 (Fig. 3IC). The absence of any significant sharp peak in the case of blank HACSNPs indicated the presence of both polymers in non-crystalline form in the structure of nanoparticles (Fig. 3ID). The presence of characteristic peaks of 5FU in the case of physical mixture of drug and blank nanoparticles (Fig. 3IE) but not in 5FU loaded HACSNPs (Fig. 3IF) indicates that drug is dispersed at a molecular level in the polymers matrix.

3.5. In vitro drug release study

As shown in Fig. 4C, in both media, about 18% of the total loaded drug was released during the first 2 h which could be considered as desorption of the drug from the surface of the nanoparticles whereas more than 70% of the total drug experienced sustained release over 30 h in both media which is attributed to the entrapped drug throughout the nanoparticles. Drug release was a little more rapid in pH 5.5. The faster release in acidic medium is in accordance with previous reports and indicates that acidic condition could increases the release efficiency of hyaluronan/chitosan based nanoparticles compared with neutral condition (Deng et al., 2014). This observation can be explained through decreasing the ionization potential of anionic polymer and interaction with positively charged groups of chitosan and also swelling of the chitosan due to strong protonation of its amine groups which accelerate the drug release. The other difference between 5FU release behavior in pH 5.5 and 7.4 is the higher total amount of released drug in pH 7.4. It seems, since 5FU has acidic properties, can be ionized in alkaline condition and its solubility may be improved in pH 7.4. This reason possibly will explain the 10% higher drug release in PBS 7.4 at the end of 30 h. Higher amounts of total released drug in higher pH was also reported for chitosan coated magnetic nanoparticles as carriers of 5FU (Zhu, Ma, Jia, Zhao, & Shen, 2009).

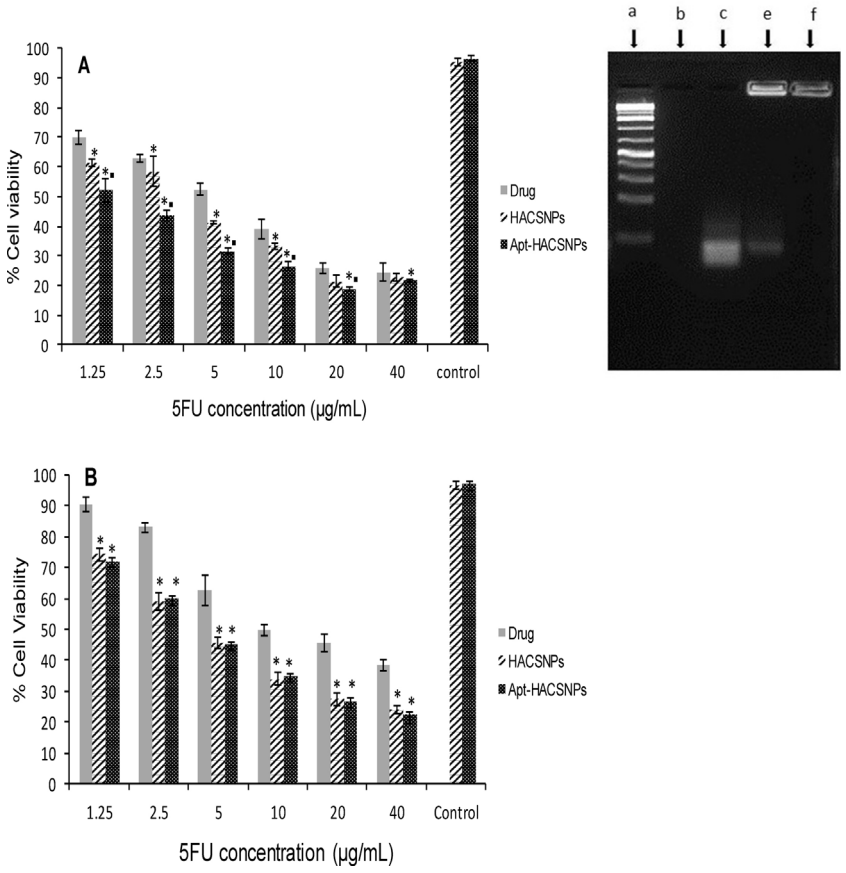

Fig. 5. *In vitro* cytotoxicity of free 5FU, 5FU loaded non-targeted and Apt-targeted HACSNPs after 48 h in (A) HT-29 and (B) CHO cell lines.* $p < 0.05$ vs free 5FU and ■ $p < 0.05$ vs non-targeted 5FU loaded HACSNPs. (mean ± S.D., $n = 3$). (C) Agarose gel electrophoresis. (a) DNA ladder, (b) HACSNPs, (c) free Apt, (d) Apt-conjugated nanoparticles before purification and (e) Apt-conjugated nanoparticles after purification.

3.6. Stability study

Stability of nanoparticles in primary aqueous suspension, PBS 7.4 and PBS 5.5 upon storage at room temperature was investigated by measuring the size, zeta potential and PDI at different time intervals. Fig. 4A and B represents the fluctuations of size and PDI in three different media, respectively. Nanoparticles showed well stability and little changes in size and PDI in primary aqueous suspension and the first signs of sedimentation were visually observed after 4 weeks of storage. Nanoparticles that were resuspended in buffered media showed less stability and more significant changes in size and PDI and precipitation occurred after 20 and 10 days of storage in PBS 7.4 and 5.5, respectively. Nanoparticles in buffered media displayed larger size and PDI at the beginning of the test that probably caused by isolation and resuspension process. One of the explanations for these differences in nanoparticles stability may be the presence of ions like CO_3^{2-}, PO_4^{2-} and H^+ in buffered media that could affect the hydration shell of counter-ions located at the nanoparticles surface and structure of water surrounding the system (Oyarzun-Ampuero, Brea, Loza, Torres, & Alonso, 2009). Zeta potential remained stable during 32, 20 and 10 days in aqueous suspension, PBS 7.4 and PBS 5.5, respectively and no significant changes were seen in three media.

3.7. Conjugation of MUC1 Apt to the surface of nanoparticles

There are several reported sequence of DNA and RNA Apts that can bind to malignant epithelial cells and MUC1 antigen. According to important role of 5FU in treatment of colorectal cancer, a comparative bibliographic study has been performed for selection of suitable Apt sequence with high selectivity and binding affinity to MUC1 expressing colorectal adenocarcinoma (Ferreira et al., 2006, 2009; Ray & White, 2010). The selected sequence with terminal NH_2 was then ordered to TAG Copenhagen Company. Agarose gel electrophoresis was applied to confirm the conjugation of MUC1-binding Apt to the surface of the HACSNPs. Fig. 6 shows the results of the agarose gel electrophoresis. HACSNPs itself did not show any band (Fig. 5Cb) while free Apt showed an obvious band on the gel (Fig. 5Cc). The band observed in loading site (Fig. 5Ce) which means Apt coupled HACSNPs cannot migrate under the applied electrophoresis condition confirms the conjugation of the Apt. Before washing, a light band corresponding to existence of unconjugated Apt was visible (Fig. 5Cd). After purification, the residual Apt was completely removed so the band of free Apt was disappeared. These data indicated the successful conjugation of Apt to the surface of HACSNPs and complete purification after centrifugation. Characterization of the Apt coupled nanoparticles have

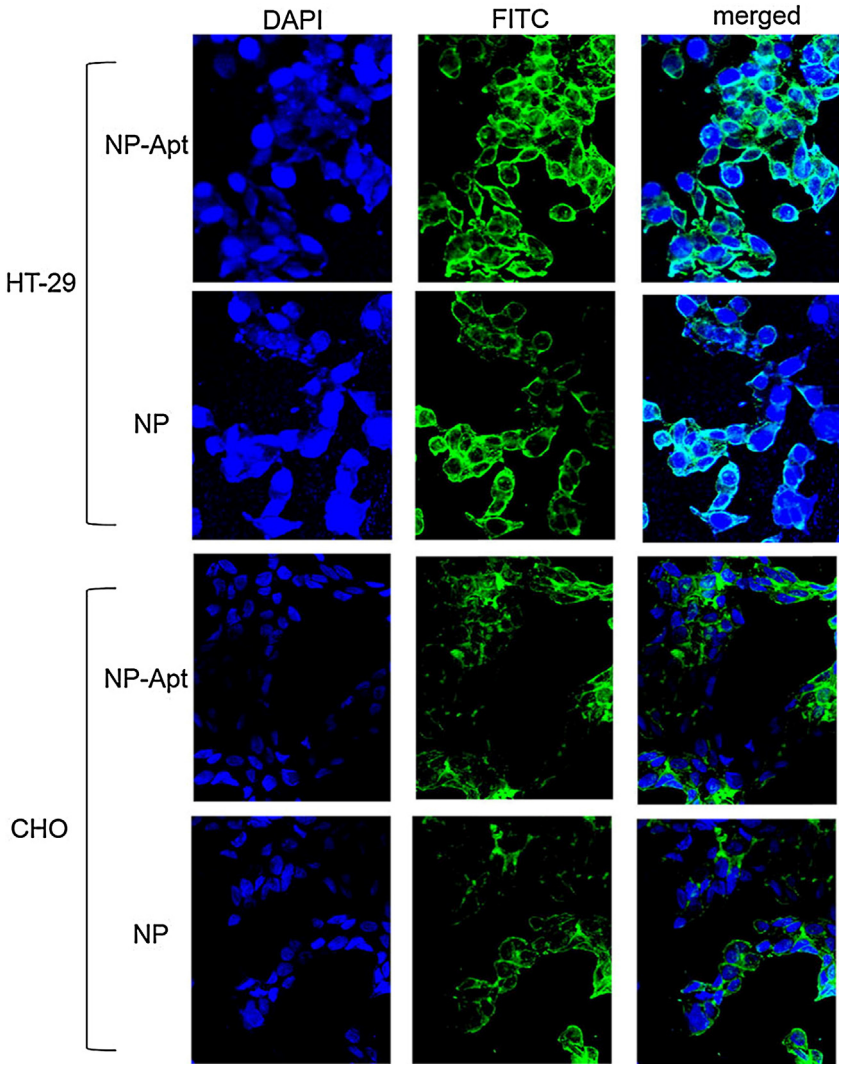

Fig. 6. Confocal fluorescent scanning microscopy (CFSM) of Apt-targeted (top row) and non-targeted (bottom row) HACSNPs in ($MUC1^+$) HT-29 and ($MUC1^-$) CHO cell lines. The right column showed the merged images of the FITC and DAPI channels.

showed a slightly increase in size (from 173 ± 2.3 to 190 ± 1.4) and PDI (from 0.084 to 0.127). A small decrease in zeta potential (from 15.33 ± 0.4 to 12.42 ± 0.3) and loading efficiency (from 45.5 ± 2.78 to 41.7 ± 1.56) have been occurred after conjugation of Apt.

3.8. Cytotoxicity assay

In vitro cytotoxicity of plain nanoparticles, free 5FU solution, non-targeted and Apt-targeted 5FU loaded HACSNPs were compared in HT-29 and CHO cell lines after 48 h incubation. Previous studies have established that HT-29 is a human colorectal adenocarcinoma cell line that overexpresses MUC1 on its surface whereas CHO is a Chinese hamster ovary cell line without MUC1 glycoprotein. The results are presented in Fig. 7. The plain nanoparticles exhibited low toxicity in both cell lines. It implied that HACSNPs could be useful as drug carriers without any significant cytotoxicity. Most differences between formulations were seen in lower concentrations where free drug had low cytotoxic effects, drug loaded nanoparticles have shown higher cytotoxicity; implying differences between internalization of drug before and after encapsulation in nanoparticles. Non-targeted nanoparticles have more cytotoxic effects than free drug in ($MUC1^+$) and ($MUC1^-$) cells and IC_{50} value showed a decrease from 5.81 ± 0.41 to 3.63 ± 0.34 in HT-29 and from 9.92 ± 0.82 to 4.16 ± 0.38 in CHO cells. This observation indicates the efficacy of HACSNPs on internalization for 5FU. Increasing the cytotoxicity of anticancer drugs including 5FU after encapsulation in polymeric carriers was reported in many studies. It has been proved that greater amount of drug could internalize into the cells in the form of nanoparticles having particle size bellow 200 nm so cells are more vulnerable to the cytotoxic effect of the drug (Arias, 2008). Accordingly, the results showed that Apt-targeted nanoparticles had more cytotoxic effect than non-targeted nanoparticles and the IC_{50} value was significantly decreased to 1.43 ± 0.42 in HT-29 ($MUC1^+$) cells ($p < 0.05$). However, cytotoxicity differences were not observed in ($MUC1^-$) cells between targeted and non-targeted nanoparticles ($p > 0.05$); suggesting that the enhanced cytotoxicity of anticancer drug has been mainly induced by the Apt. Improving the efficacy of Apt-conjugated nanoparticles against prostate cancer and glioma brain tumors were also reported in previous drug delivery studies (Guo et al., 2011). It is assumed that Apt possibly promoted the interaction between nanoparticles and receptor-overexpressing cells via ligand–receptor recognition. In CHO ($MUC1^-$) cells, Apt did not improve the interaction between nanoparticles and cells as a result failed to enhance the uptake and cytotoxicity of nanoparticles.

3.9. In vitro cellular uptake

In another attempt the interaction between nanoparticles and the target cells was investigated employing confocal fluorescent scanning microscopy (CFSM) after 2 h incubation of cumarin-6 loaded targeted and non-targeted nanoparticles with ($MUC1^+$) and ($MUC1^-$) cells. Obtained images indicate that the highest accumulation was seen in ($MUC1^+$) cells incubated with Apt-targeted nanoparticles (Fig. 8). As it is demonstrated, uptake of the nanoparticles by HT-29 cells was significantly enhanced when the nanoparticles were decorated with MUC1 Apt in comparison to the non-targeted nanoparticles supporting again that the Apt facilitated the uptake of nanoparticles by the cells. Other studies on effect of MUC1-binding Apt on targeted delivery of chemotherapeutics to ($MUC1^+$) breast cancer cells also demonstrated higher uptake of Apt-labeled formulations by MUC1 overexpressing cells. It seems that bounded Apt acts like an anchor and pulls the nanoparticles to the vicinity of the cell, and improves the chance of the nanoparticles being internalized by receptor-positive cells. In contrast, as CHO cells do not express MUC1 glycoprotein, really there has not been any difference between non-targeted and Apt-targeted nanoparticles. These finding confirms the results of the cytotoxicity assays and indicates that targeted nanoparticles can effectively enter and distribute in the cellular cytoplasm with acceptable specificity and selectivity. As a result, it can be proposed that the currently developed Apt-targeted nanoparticles can achieve higher internalization and cytotoxicity in colorectal adenocarcinoma tumor cells.

4. Conclusion

A new Apt-targeted HACSNPs loaded with 5FU for active targeting of MUC1 overexpressing adenocarcinomas was successfully designed and characterized. Small size, narrow size distribution, long term stability, sustained drug release behavior and higher cytotoxicity of 5FU loaded HACSNPs in comparison with conventional drug demonstrated the remarkable capabilities of HACSNPs as drug carrier. Higher *in vitro* cytotoxicity and significant greater cellular uptake of Apt-targeted formulation in MUC1 overexpressing cells were proved by a series of MTT assays and CFSM studies. According to the results achieved in these studies, the novel Apt-targeted HACSNPs can effectively enhance the delivery of 5FU to HT-29 colorectal adenocarcinoma cells. Therefore, it can be proposed that MUC1 targeted HACSNPs can possess higher anticancer therapeutic efficacy through colorectal malignant cells rather than normal cells and probably could reduce side effect of the therapies.

Acknowledgments

This study was granted by Iran National Science Foundation (INSF).

References

Arias, J. L. (2008). Novel strategies to improve the anticancer action of 5-fluorouracil by using drug delivery systems. *Molecules*, *13*(10), 2340–2369.

Bae, Y. H., & Park, K. (2011). Targeted drug delivery to tumors: Myths, reality and possibility. *Journal of Controlled Release*, *153*(3), 198.

Bertrand, N., Wu, J., Xu, X., Kamaly, N., & Farokhzad, O. C. (2014). Cancer nanotechnology: The impact of passive and active targeting in the era of modern cancer biology. *Advanced Drug Delivery Reviews*, *66*, 2–25. http://dx.doi.org/10.1016/j.addr.2013.11.009

Chang, K., Pi, Y., Lu, W., Wang, F., Pan, F., Li, F., et al. (2014). Label-free and high-sensitive detection of human breast cancer cells by aptamer-based leaky surface acoustic wave biosensor array. *Biosensors and Bioelectronics*, *60*, 318–324.

Deng, X., Cao, M., Zhang, J., Hu, K., Yin, Z., Zhou, Z., et al. (2014). Hyaluronic acid–chitosan nanoparticles for co-delivery of MiR-34a and doxorubicin in therapy against triple negative breast cancer. *Biomaterials*, *35*(14), 4333–4344. http://dx.doi.org/10.1016/j.biomaterials.2014.02.006

Dhar, S., Gu, F. X., Langer, R., Farokhzad, O. C., & Lippard, S. J. (2008). Targeted delivery of cisplatin to prostate cancer cells by aptamer functionalized Pt(IV) prodrug-PLGA-PEG nanoparticles. *Proceeding of the National Academy of Science of United States of America*, *105*(45), 17356–17361. http://dx.doi.org/10.1073/pnas.0809154105

Duceppe, N., & Tabrizian, M. (2009). Factors influencing the transfection efficiency of ultra low molecular weight chitosan/hyaluronic acid nanoparticles. *Biomaterials*, *30*(13), 2625–2631. http://dx.doi.org/10.1016/j.biomaterials.2009.01.017

Duncan, R. (2003). The dawning era of polymer therapeutics. *Nature Reviews Drug Discovery*, *2*(5), 347–360. http://dx.doi.org/10.1038/nrd1088

Farokhzad, O. C., Cheng, J., Teply, B. A., Sherifi, I., Jon, S., Kantoff, P. W., et al. (2006). Targeted nanoparticle-aptamer bioconjugates for cancer chemotherapy in vivo. *Proceedings of the National Academy of Sciences of United States of America*, *103*(16), 6315–6320.

Ferreira, C. S., Cheung, M. C., Missailidis, S., Bisland, S., & Gariepy, J. (2009). Phototoxic aptamers selectively enter and kill epithelial cancer cells. *Nucleic Acids Research*, *37*(3), 866–876. http://dx.doi.org/10.1093/nar/gkn967

Ferreira, C. S., Matthews, C. S., & Missailidis, S. (2006). DNA aptamers that bind to MUC1 tumour marker: Design and characterization of MUC1-binding single-stranded DNA aptamers. *Tumour Biology*, *27*(6), 289–301. http://dx.doi.org/10.1159/000096085

Guo, J., Gao, X., Su, L., Xia, H., Gu, G., Pang, Z., et al. (2011). Aptamer-functionalized PEG-PLGA nanoparticles for enhanced anti-glioma drug delivery. *Biomaterials*, *32*(31), 8010–8020. http://dx.doi.org/10.1016/j.biomaterials.2011.07.004

Jarmila, V., & Vavrikova, E. (2011). Chitosan derivatives with antimicrobial, antitumour and antioxidant activities—A review. *Current Pharmaceutical Design*, *17*(32), 3596–3607.

Li, P., Wang, Y., Peng, Z., She, F., & Kong, L. (2011). Development of chitosan nanoparticles as drug delivery systems for 5-fluorouracil and leucovorin blends. *Carbohydate Polymers*, *85*(3), 698–704.

Mok, H., Park, J. W., & Park, T. G. (2007). Antisense oligodeoxynucleotide-conjugated hyaluronic acid/protamine nanocomplexes for intracellular gene inhibition. *Bioconjugate Chemistry*, *18*(5), 1483–1489.

Muzzarelli, C., Stanic, V., Gobbi, L., Tosi, G., & Muzzarelli, R. A. (2004). Spray-drying of solutions containing chitosan together with polyuronans and characterisation of the microspheres. *Carbohydate Polymers*, *57*(1), 73–82.

Muzzarelli, R. A., Greco, F., Busilacchi, A., Sollazzo, V., & Gigante, A. (2012). Chitosan, hyaluronan and chondroitin sulfate in tissue engineering for cartilage regeneration: A review. *Carbohydate Polymers*, *89*(3), 723–739.

Muzzarelli, R. A., Lough, C., & Emanuelli, M. (1987). The molecular weight of chitosans studied by laser light-scattering. *Carbohydrate Research*, *164*, 433–442.

Nizri, G., Magdassi, S., Schmidt, J., Cohen, Y., & Talmon, Y. (2004). Microstructural characterization of micro- and nanoparticles formed by polymer-surfactant interactions. *Langmuir*, *20*(11), 4380–4385.

Oyarzun-Ampuero, F. A., Brea, J., Loza, M. I., Torres, D., & Alonso, M. J. (2009). Chitosan-hyaluronic acid nanoparticles loaded with heparin for the treatment of asthma. *International Journal of Pharmaceutics*, *381*(2), 122–129. http://dx.doi.org/10.1016/j.ijpharm.2009.04.009

Ray, P., & White, R. R. (2010). Aptamers for targeted drug delivery. *Pharmaceuticals*, *3*(6), 1761–1778.

Sayari, E., Dinarvand, M., Amini, M., Azhdarzadeh, M., Mollarazi, E., Ghasemi, Z., et al. (2014). MUC1 aptamer conjugated to chitosan nanoparticles, an efficient targeted carrier designed for anticancer SN38 delivery. *International Journal of Pharmaceutics*, *473*(1-2), 304–315.

Umerska, A., Paluch, K. J., Inkielewicz-Stepniak, I., Santos-Martinez, M. J., Corrigan, O. I., Medina, C., et al. (2012). Exploring the assembly process and properties of novel crosslinker-free hyaluronate-based polyelectrolyte complex nanocarriers. *International Journal of Pharmaceutics*, *436*(1–2), 75–87. http://dx.doi.org/10.1016/j.ijpharm.2012.07.011

Zhu, L., Ma, J., Jia, N., Zhao, Y., & Shen, H. (2009). Chitosan-coated magnetic nanoparticles as carriers of 5-fluorouracil: Preparation, characterization and cytotoxicity studies. *Colloids and Surfaces B: Biointerfaces*, *68*(1), 1–6. http://dx.doi.org/10.1016/j.colsurfb.2008.07.020